Journal of Statistical Physics, Vol. 107, Nos. 1/2, April 2002 (© 2002)

Simulation of Combustion Field with Lattice Boltzmann Method

Kazuhiro Yamamoto,[1, 2] Xiaoyi He,[2] and Gary D. Doolen[2]

Received February 13, 2001; accepted November 9, 2001

Turbulent combustion is ubiquitously used in practical combustion devices. However, even chemically non-reacting turbulent flows are complex phenomena, and chemical reactions make the problem even more complicated. Due to the limitation of the computational costs, conventional numerical methods are impractical in carrying out direct 3D numerical simulations at high Reynolds numbers with detailed chemistry. Recently, the lattice Boltzmann method has emerged as an efficient alternative for numerical simulation of complex flows. Compared with conventional methods, the lattice Boltzmann scheme is simple and easy for parallel computing. In this study, we present a lattice Boltzmann model for simulation of combustion, which includes reaction, diffusion, and convection. We assume the chemical reaction does not affect the flow field. Flow, temperature, and concentration fields are decoupled and solved separately. As a preliminary simulation, we study the so-called "counter-flow" laminar flame. The particular flow geometry has two opposed uniform combustible jets which form a stagnation flow. The results are compared with those obtained from solving Navier–Stokes equations.

KEY WORDS: Lattice Boltzmann method; combustion; premixed flame; chemical reaction.

1. INTRODUCTION

Turbulent combustion is present in most combustion devices. Under practical conditions, turbulence is a complex three-dimensional phenomenon. In combustion processes, many reactions between stable species and radicals occur.[1, 2] These chain reactions consist of a series of consecutive, competitive, and opposing reactions with different reaction rate constants.

[1] Mechanical Engineering, Toyohashi University of Technology, 1-1 Tempaku, Hibarigaoka, Toyohashi, Aichi 441-8580, Japan; e-mail: yamamoto@mech.tut.ac.jp
[2] Theoretical Division, Los Alamos National Laboratory, Los Alamos, New Mexico 87545.

0022-4715/02/0400-0367/0 © 2002 Plenum Publishing Corporation

These chemical reactions make the problem quite more complicated, and it is often crucial to include the detailed chemistry and the three-dimensional behavior of turbulent combustion. Due to the limitation of computational costs, conventional numerical methods are impractical in carrying out direct numerical simulations.

Recently, the lattice Boltzmann method (LBM) has emerged as an efficient alternative for numerical simulation.[3] For example, He and Doolen have simulated the flow around two-dimensional circular cylinder to show the time evolution of vortex shedding.[4] Martinez *et al.* have examined the turbulence in shear layer, and the turbulent flow can be well simulated at a relatively high Reynolds number of 10,000.[5] Compared with conventional methods, the lattice Boltzmann scheme is simple and easy for parallel computing. It has been used for direct numerical simulation (DNS). Therefore, combustion field can be simulated if the reaction term is well described.

The reactive flow has been simulated in several studies by using LBM. For example, Chen *et al.* have examined the effect of fluid flow on chemical reaction on solid surfaces to study geochemical process including dissolution and precipitation.[6] Recently, some groups have tried combustion simulation using special treatment for chemical reaction. Succi *et al.*[7] have adapted the conserved scalar approach with fast-chemistry assumption where reaction is fast in comparison with turbulent mixing processes. In this case, they don't have to solve combustion field directly, and temperature and concentration fields are determined by one parameter, mixture fraction.[8] This technique is only valid for a non-premixed flame at moderate and high Reynolds numbers. Then, a methane/air diffusion flame is simulated by simple extension of the Lattice Boltzmann equation to obtain mixture fraction. On the other hand, Filippova *et al.* have presented a new approach for low Mach number combustion.[9] The flow field is solved by LBM, and transport equations for energy and species are solved by a finite difference scheme. Their model can handle variable density, which is usually important factor in combustion problem. They have focused on a diffusion flame formed around a porous cylinder burner. However, they have used artificial mixture and reaction. Also, LB equations and other conservation equations must be coupled in non-dimensional coordinate.

In this study, we will present a lattice Boltzmann model for simulation of combustion. We solve the flow, temperature, and concentration fields using LB equations only. For simplicity, we assume the chemical reaction does not affect the flow field. Thus, all fields are decoupled and solved separately. The model includes reaction, diffusion, and convection. As a preliminary simulation, we study the so-called "counter-flow" laminar flame.

This configuration is considered to occur in turbulent combustion.[10–14] The particular flow geometry is composed of two opposed combustible uniform jets to form a stagnation flow. The twin flames are formed in this counter flow. Since this flame is well understood, it is appropriate for benchmark study. The results are compared with those obtained by conventional scheme from solving Navier–Stokes equations. Also, the counter-flow flame is simulated by compressible Navier–Stokes model to discuss the variable density effect.

2. MODEL AND ASSUMPTION

The lattice Boltzmann method has been recognized as an efficient alternative for numerical simulation of fluid flow. For simulation of combustion field, the model must include the reaction term describing heat release and mass rate of production. In this section, we explain the numerical scheme and assumptions. To verify the LBM model, we also simulate combustion field by the conventional method which consists of conservation equations of mass, momentum, energy, and species. The governing equations for each method are shown in the next session.

We focus on the counter-flow premixed flame. Figure 1 shows the schematics of this flame formed in counter flow. Two-dimensional rectangular coordinates are used. Two parallel stationary walls are located at $y = -L$ and L, where L is the half-length of the distance between walls. The combustible mixture is uniformly ejected from the top and bottom walls, and it reacts in the reaction zone. Then, two flames are formed in this flow. The burned gas flows outward along the x-direction.

The fuel is propane. The following assumptions are made:

1. The flow is symmetric, and there are no external forces.
2. The chemical reaction does not affect the flow field in an incompressible model.
3. The transport properties are constant.
4. The diffusion obeys the Fick's law of diffusion.
5. The reaction is expressed with an over-all one step reaction,

$$C_3H_8 + 5O_2 \rightarrow 3CO_2 + 4H_2O, \qquad \omega_{ov} = k_{ov} C_{C_3H_8} C_{O_2} \exp(-E/RT)$$

where C_i is molar concentration. Mass rate of production for species i is obtained by this over-all reaction rate. The reaction coefficient, k_{ov}, and the effective activation energy, E, are referred to refs. 14 and 15. Nitrogen is assumed to be inert.

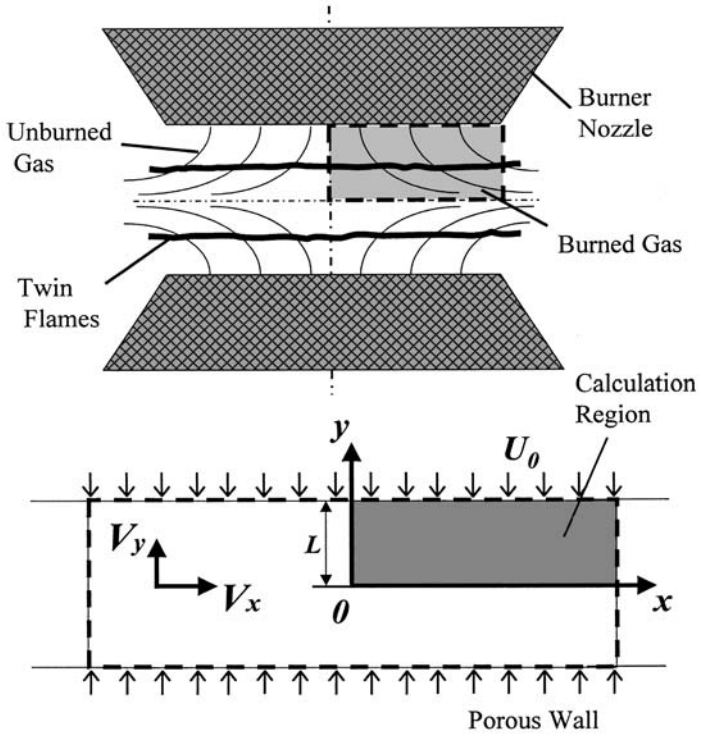

Fig. 1. Counter flow and coordinate.

6. The heat of formations for the species are adopted from the Joint Army-Navy-Air Force (JANAF) thermochemical tables.[16] The various diffusion coefficients, which are used to evaluate the collision relaxation time, are determined using a rigorous treatment of kinetic theory.[17]

7. Viscous energy dissipation and radiative heat loss are neglected.

For the stagnation lines at $x = 0$ and $y = 0$, we assume the flow is symmetrical. Then, the calculation region is $x \geqq 0$ and $y \geqq 0$.

3. GOVERNING EQUATION

3.1. Lattice Boltzmann Method

We use an incompressible 2D square Lattice BGK model (d2q9).[18] The relaxation time for flow, temperature, and species are respectively fixed, because transport coefficients, such as kinetic viscosity and diffusion

coefficient, are constant. We assume the chemical reaction does not affect the flow field for simplicity. Flow, temperature, and concentration fields are decoupled and solved separately. Formula of LBM scheme for flow, temperature, and concentration fields are shown separately as following.

3.1.1. Flow Field

The 9-bit lattice BGK model evolves on the two-dimensional square lattice space with the following 9 discrete velocities:[18]

$$\begin{aligned}
\mathbf{e}_\alpha &= (0, 0) && \alpha = 0 \\
&= (\cos[(\alpha-1)\,\pi/2],\ \sin[(\alpha-1)\,\pi/2])\cdot c && \alpha = 1\text{–}4 \\
&= (\cos[(\alpha-5)\,\pi/2+\pi/4], \sin[(\alpha-5)\,\pi/2+\pi/4])\,\sqrt{2}\cdot c && \alpha = 5\text{–}8
\end{aligned}$$

where c is the advection speed. For the incompressible fluid, the evolution equation using the pressure distribution function is

$$p_\alpha(\mathbf{x}+\mathbf{e}_\alpha\delta_t, t+\delta_t) - p_\alpha(\mathbf{x}, t) = -\frac{1}{\tau}\left[p_\alpha(\mathbf{x}, t) - p_\alpha^{\mathrm{eq}}(\mathbf{x}, t)\right]$$

where δ_t is the time step. The equilibrium distribution function, p_α^{eq}, is given by

$$p_\alpha^{\mathrm{eq}} = w_\alpha\left\{p + p_0\left[3\frac{(\mathbf{e}_\alpha\cdot\mathbf{u})}{c^2} + \frac{9}{2}\frac{(\mathbf{e}_\alpha\cdot\mathbf{u})^2}{c^4} - \frac{3}{2}\frac{\mathbf{u}^2}{c^2}\right]\right\}$$

where $w_\alpha = 4/9$, $w_\alpha = 1/9$ $(\alpha = 1:4)$, $w_\alpha = 1/36$ $(\alpha = 5:8)$. The sound speed, c_s, is $c/\sqrt{3}$, and $p_0 = \rho_0 c_s^2$, where ρ_0 is constant density in the incompressible model. The pressure, p, and the velocity, $\mathbf{u} = (v_x, v_y)$, are calculated by

$$p = \sum_\alpha p_\alpha, \qquad p_0\mathbf{u} = \sum_\alpha p_\alpha\mathbf{e}_\alpha$$

Through the Chapman–Enskog procedure, the incompressible Navier–Stokes equations are derived from these equations. The kinetic viscosity, v, is

$$v = \frac{2\tau-1}{6}c^2\delta_t$$

3.1.2. Temperature and Concentration Fields

For combustion simulation, we introduce the LBM formula for temperature and concentration fields as follows:

$$F_{s,\alpha}(\mathbf{x}+\mathbf{e}_\alpha\delta_t, t+\delta_t)-F_{s,\alpha}(\mathbf{x}, t)$$
$$= -\frac{1}{\tau_s}[F_{s,\alpha}(\mathbf{x}, t)-F^{\mathrm{eq}}_{s,\alpha}(\mathbf{x}, t)]+w_\alpha Q_s,$$
$$s = T, Y_i \quad (i = \mathrm{C_3H_8}, \mathrm{O_2}, \mathrm{CO_2}, \mathrm{H_2O})$$

The equilibrium distribution functions are given by

$$F^{\mathrm{eq}}_{s,\alpha} = w_\alpha s\left\{1+3\frac{(\mathbf{e}_\alpha\cdot\mathbf{u})}{c^2}+\frac{9}{2}\frac{(\mathbf{e}_\alpha\cdot\mathbf{u})^2}{c^4}-\frac{3}{2}\frac{\mathbf{u}^2}{c^2}\right\}$$

The temperature, T, and mass fraction of species i, Y_i, are obtained in terms of the distribution function by

$$T=\sum_\alpha F_{T,\alpha}, \qquad Y_i=\sum_\alpha F_{Y_i,\alpha}$$

The source term due to chemical reaction, Q_s, is given by the similarity in non-dimensional equations of temperature and concentration fields. The mass rate of production for species i [kg/m^{3}s] appearing in the conservation equation of species is,

$$\omega_i = a_i\cdot M_i\cdot\omega_{\mathrm{ov}} = a_i\cdot M_i\cdot k_{\mathrm{ov}}C_{\mathrm{C_3H_8}}C_{\mathrm{O_2}}\exp(-E/RT)$$

where ω_{ov} is the over-all reaction rate [mol/m^{3}s] and M_i is the molecular weight of species i [kg/mol]. Stoichiometric coefficients, a_i, are $a_{\mathrm{C_3H_8}} = -1$, $a_{\mathrm{O_2}} = -5$, $a_{\mathrm{CO_2}} = 3$, and $a_{\mathrm{H_2O}} = 4$, respectively. All reaction parameters of this simplified reaction are evaluated in the compressible model to reproduce experimental data.[14, 15] Hence, the correction is needed for heat expansion even in the incompressible model; otherwise the reaction rate is extremely overestimated. Here, to obtain the reaction rate, the molar concentration of propane or oxygen is determined by

$$C_i = \frac{\rho_0 Y_i}{M_i}\cdot\left(\frac{T_0}{T}\right)$$

where ρ_0 is the constant density of room temperature, T_0, and T is the local temperature. The reaction rate is non-dimensionalized by the density, characteristic length, L, and velocity, U_0. By the similarity in lattice space and real coordinate, the reaction rate in LBM is,

$$(\omega_i)_{\mathrm{LBM}} = \frac{\omega_i}{\rho_0 U_0/L}\cdot\left(\frac{\rho_0 U_0}{L}\right)_{\mathrm{LBM}}$$

The thermal diffusivity, κ, and diffusion coefficient, D_i, are given by

$$\kappa = \frac{2\tau_T - 1}{6} c^2 \delta_t, \qquad D_i = \frac{2\tau_{Y_i} - 1}{6} c^2 \delta_t$$

3.2. Conventional Method

To confirm results by LBM, we also simulate combustion field by conventional scheme. It is to solve differential equations maintaining conservation of mass, momentum, energy, and species. These governing equations describe convective motion of fluid, chemical reactions among the constituent species, and diffusive transport process such as thermal conduction and molecular diffusion. To consider the compressible effect neglected in LB scheme, we use both compressible and incompressible models. The equations for the compressible model are explained in this section, while those of the incompressible model are obtained when the density is set to be constant. The approach is to solve a set of time-dependent, coupled partial differential equations with a finite difference method.[14] Assuming that the quantities are known at a time level t^n, the solution at a new level t^{n+1} is obtained by using the Crank–Nicholson method. This procedure is continued until a steady solution is obtained. The algebraic equations yielded from discretization are solved by the Gauss–Seidel method.

3.2.1. Stream Function and Velocity

$$u = \frac{1}{\rho}\frac{d\varphi}{dy}, \qquad v = -\frac{1}{\rho}\frac{d\varphi}{dx}$$

where φ is the stream function to satisfy the conservation equation of mass (equation of continuity).

3.2.2. Vorticity Equation

$$\frac{\partial W}{\partial t} + v_x \frac{\partial W}{\partial x} + v_y \frac{\partial W}{\partial y} = -W\left(\frac{\partial v_x}{\partial x} + \frac{\partial v_y}{\partial y}\right) + \frac{\mu}{\rho}\left(\frac{\partial^2 W}{\partial x^2} + \frac{\partial^2 W}{\partial y^2}\right) - \frac{1}{\rho}\frac{\partial \rho}{\partial x}\left(v_x \frac{\partial v_y}{\partial x} + v_y \frac{\partial v_y}{\partial y}\right) + \frac{1}{\rho}\frac{\partial \rho}{\partial y}\left(v_x \frac{\partial v_x}{\partial x} + v_y \frac{\partial v_x}{\partial y}\right)$$

$$W = \frac{\partial v_y}{\partial x} - \frac{\partial v_x}{\partial y}$$

where W [1/s] is the vorticity. The viscosity, μ, is constant and the kinetic viscosity is obtained by $\nu = \mu/\rho$.

3.2.3. Energy Equation

$$\frac{\partial T}{\partial t} + v_x \frac{\partial T}{\partial x} + v_y \frac{\partial T}{\partial y} = \frac{\lambda}{\rho C_p}\left(\frac{\partial^2 T}{\partial x^2} + \frac{\partial^2 T}{\partial y^2}\right) + \frac{Q \cdot \omega_{ov}}{\rho \cdot C_p}$$

where Q [J/mol] is the heat of over-all reaction. The heat capacity, C_p [J/kg·K], and the thermal conductivity, λ [J/m·s·K], are also constant. Thermal diffusivity, κ [m^2/s], is obtained by $\kappa = \lambda/(\rho \cdot C_p)$.

3.2.4. Species Conservation

$$\rho\left(\frac{\partial Y_i}{\partial t} + v_x \frac{\partial Y_i}{\partial x} + v_y \frac{\partial Y_i}{\partial y}\right)$$
$$= D_i \frac{\partial}{\partial x}\left(\rho \frac{\partial Y_i}{\partial x}\right) + D_i \frac{\partial}{\partial y}\left(\rho \frac{\partial Y_i}{\partial y}\right) + \omega_i, \qquad i = C_3H_8, O_2, CO_2, H_2O$$

where ω_i [kg/m^{3}s] is the mass rate of production for species i, and D_i is the diffusion coefficient. Nitrogen is taken as inert and its mass fraction is obtained by

$$Y_{N_2} = 1 - \sum_{i \neq N_2} Y_i$$

This approach is attractive in problems having one species, nitrogen in this calculation, is always present in excess to ensure that total diffusion flux is zero.[19]

3.2.5. Equation of State

In the compressible model, we use the following equation of state for the mixture.

$$\rho = p \Big/ \left\{ R_u T \sum_i (Y_i/M_i) \right\}$$

where R_u is the universal gas constant (8.315 J/mol·K). The static pressure is obtained by solving the Poisson-equation of pressure derived using the conservation of momentum.

3.2.6. Equivalence Ratio

It is useful to define the equivalence ratio to know the properties of premixed mixtures, which is obtained by the ratio of the actual fuel-air mass ratio to the ratio $(F/A)_{st}$ for a stoichiometric process.[8] The stoichiometric reaction is defined as a unique reaction in which all the reactants are consumed. When the fuel is propane, the stoichiometric process is $C_3H_8 + 5O_2 \rightarrow 3CO_2 + 4H_2O$, and the equivalence ratio by using mass fraction of propane and air, ϕ, is

$$\phi = \frac{(F/A)}{(F/A)_{st}} = \frac{Y_{C_3H_8}/Y_{air}}{(1 \cdot M_{C_3H_8})/(5 \cdot M_{O_2}/Y_{O_2,0})} = \frac{Y_{C_3H_8}/(1-Y_{C_3H_8})}{0.0642}$$

where the molecular weights of propane and oxygen are 44.1 and 32.0 g/mol, and $Y_{O_2,0}(=0.233)$ is the mass fraction of oxygen in the air. For fuel-lean conditions, we have $0 < \phi < 1$, for stoichiometric conditions, we have $\phi = 1$, and for fuel-rich conditions, we have $1 < \phi < \infty$. In this calculation, we only use a lean mixture. Propane and oxygen concentration, which is needed for calculating the reaction rate, are obtained by $C_i = \rho Y_i / M_i$.

3.3. Boundary Conditions and Parameters

Both stagnation lines of $x = 0$ and $y = 0$, we use the symmetric conditions for conventional model, and those are bounce-back scheme for LB method. At the wall (inlet), the velocity, U_0, is 0.2 m/s, temperature, T_0, is room temperature ($=300$ K), and concentration are those of unburned mixture. For LBM, the inflow boundary is adopted for pressure, and hydrodynamic condition for temperature and concentration.[20] At the outlet, the pressure is constant and the developed boundary condition is used for temperature and concentration. The half-length of the distance between walls, L, is 10 mm, and longitude length is 16.7 mm. Then, its Reynolds number $(=\rho_0 L/\nu)$ is 124. The number of grids is $301(N_x) \times 181(N_y)$, and the mesh size is about 0.05 mm, so as to represent the flame structure accurately.

Other parameters used in the calculation are as follows; reaction coefficient, k_{ov}, is 9.9×10^{13} [cm^3/mol·s], effective activation energy, E, is 30 [kcal/mol], kinetic viscosity is 1.6×10^{-5} [m^2/s], heat of overall reaction, Q is 2.05×10^6 [J/mol], thermal diffusivity, κ, is 2.2×10^{-5} [m^2/s], and heat capacity C_p is 1.01×10^3 [J/kg·K]. Diffusion coefficients for each species are taken as $D_{C_3H_8} = 1.1 \times 10^{-5}$ [m^2/s], $D_{O_2} = 2.1 \times 10^{-5}$ [m^2/s], $D_{CO_2} = 1.6 \times 10^{-5}$ [m^2/s], $D_{H_2O} = 2.2 \times 10^{-5}$ [m^2/s].

4. RESULTS AND DISCUSSION

4.1. Flow Field

First, we show the flow field where counter-flow flames are formed. Before that, we have conducted convergent study to choose the proper calculation domain. In LB calculation, the velocity at the wall is 0.1. The pressure at the outlet is 1/3. The density is 1 and the Reynolds number is kept constant of Re = 124. Table I shows the results for different grid system with similarity. The maximum of both pressure, p, and velocity, v_x, are examined. For flow field, the grid number of $151(N_x) \times 91(N_y)$ is enough, but we use more grids to describe thin reaction zone.[14] We compare these results with that by conventional method. Figure 2 shows the distribution of velocities of v_x at $y=0$ and v_y at $x=0$, respectively. The velocity is normalized to the inlet velocity at the wall, U_0. Both results show good agreement, though v_x by LBM is slightly higher. This may be caused by the slip boundary condition at $y=0$ in LBM, which differs to the symmetric condition adopted in conventional simulation. The flow field is well simulated in the case of counter flow.

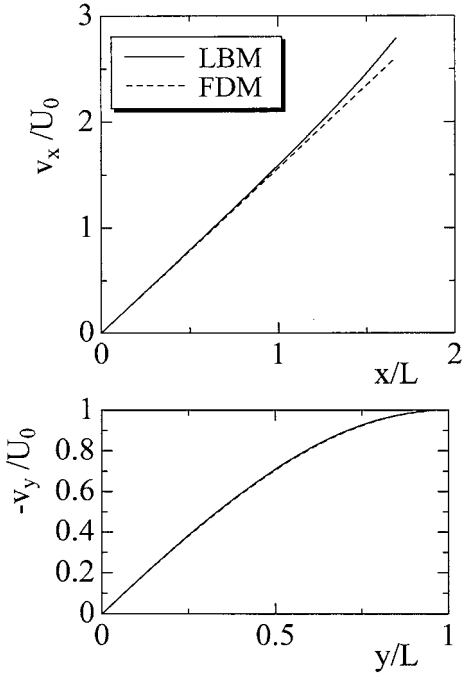

Fig. 2. Distributions of non-dimensional velocities of v_x and v_y; Re = 124.

Table I. Computational Domain in the Converge Study

(N_x, N_y)	τ	$P_{\max}(p(0, 0))$	$v_{x,\max}(v_x(0, 1.67L))$
(31, 19)	0.544	—	—
(51, 31)	0.572	0.489	0.483
(101, 61)	0.645	0.372	0.278
(151, 91)	0.717	0.371	0.275
(301, 181)	0.935	0.371	0.275

4.2. Temperature and Concentration Field

Next, we investigate the temperature and concentration fields. Before that, we calculate the combustion field in simple flow to confirm that reaction scheme is well described. We simulate the flame formed in uniform flow using d2q9 LB model. The inlet velocity is uniform in the y-direction, and both upper and lower boundaries have free slip boundary conditions, obtaining the uniform flow field in the whole domain. The number of grid points is $501(N_x) \times 3(N_y)$, so as to analyze the flame behavior like one-dimensional planar waves. Initially, the region of high temperature, the *adiabatic flame temperature*[8] for example, is given to ignite the mixture, and the flame (reaction region) propagates in the flow direction (x-direction). The periodic boundary condition at the upper and lower walls is also used, but little difference is recognized. Here, we estimate the burning velocity, which is usually defined as the flow velocity if the flame is stationary in one-dimensional consideration.[8]

Figure 3 shows the profiles of mass rate of production for propane at different time steps. Those are non-dimensionalized by

$$\omega_{\mathrm{N},\,\mathrm{C_3H_8}} = \frac{\omega_{\mathrm{C_3H_8}}}{\rho_0 U_{\mathrm{in}}/L}$$

The equivalence ratio, ϕ, is 0.6, and the density is about 1.1 kg/m^3. The inlet velocity, U_{in}, is 1 m/s and the channel length is 0.1 m. In LB model, the inlet velocity and the density are 0.1 and 1, respectively. The inlet is located at $IX = 1$ ($x = 0$), where IX is the grid point in the flow direction. The region of high temperature is given at $IX < 50$ initially ($time = 0$). As seen in this figure, the flame moves downstream. This is because the flow velocity is much larger than the burning velocity. Figure 4 shows the flame position, which is defined by location where the reaction rate takes its maximum. It is found that the flame propagates at same speed. The grid number in the cross channel direction, N_y, is increased up to 101, but the

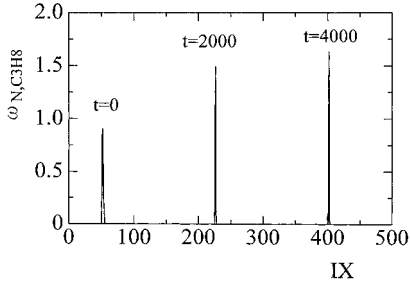

Fig. 3. Profiles of mass rate of production for propane in uniform flow of $\phi = 0.6$; $t = 0$, 2000, and 4000.

dependence of the flame speed on the channel width is not observed. Since the flame propagation speed, V_f, is equal to the inlet velocity subtracted by the burning velocity, the burning velocity can be estimated by $S_L = U_{\text{in}} - V_f$. Based on the similarity between lattice space of LBM and real coordinate, the burning velocity is given by the following equation,

$$S_L = \left(\frac{S_L}{U_{\text{in}}}\right)_{\text{LBM}} \cdot U_{\text{in}} = \left(\frac{U_{\text{in}} - V_f}{U_{\text{in}}}\right)_{\text{LBM}} \cdot U_{\text{in}}$$

The resultant burning velocity is 0.12 m/s. The experimentally obtained burning velocity is 0.11 m/s.[21] It appears that the reaction term is well described in LB model.

Next, we show some results of the counter-flow flame. To explain the flame and flow configurations, the flow field and reaction zone are shown in Fig. 5 with velocity vectors. The equivalence ratio is 0.6. The unburned

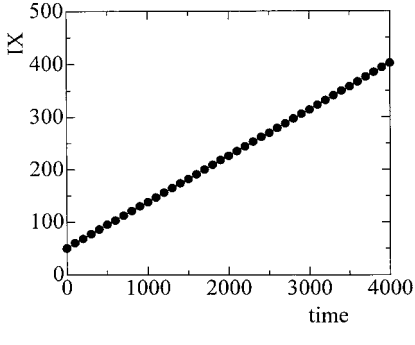

Fig. 4. Position of reaction zone, $U_{\text{in}} = 0.1$, $\phi = 0.6$.

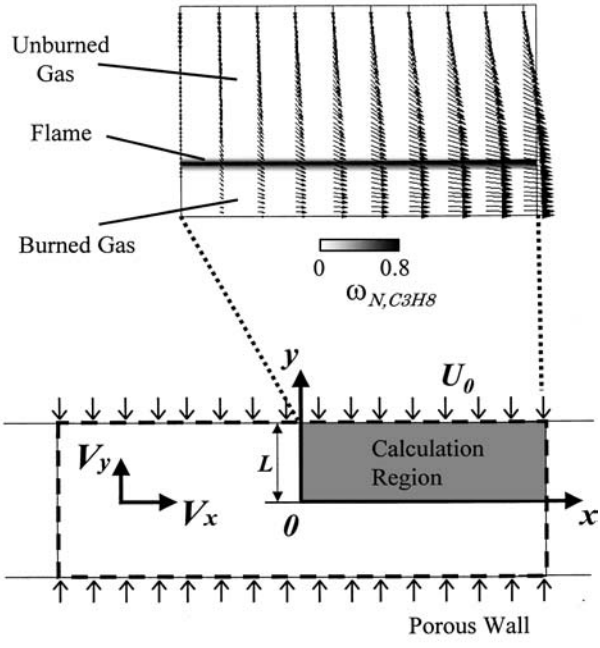

Fig. 5. Flame and flow configurations; $\phi = 0.6$.

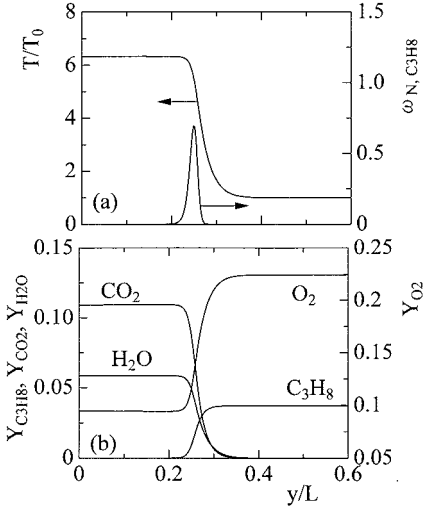

Fig. 6. Distributions of (a) temperature and mass rate of production for propane, (b) mass fraction of species; $\phi = 0.6$, Re = 124.

gas is ejected from the porous wall, and reacts in the flame zone, and finally it becomes burned gas. The temperature is almost constant along the x-axis. Figure 6 shows the temperature and concentration distributions at $x=0$. The mass rate of production for propane is also shown. In Fig. 6a, as the center is approached, the temperature starts to increase at $y/L \simeq 0.3$, and steeply increases at $y/L = 0.2$–0.3. The reaction zone is located in this region, where the large heat release occurs to cause the temperature increase. Then, temperature becomes constant in the burned gas region.

Figure 6b shows the mass fraction profiles. As seen in this figure, the reactants, C_3H_8 and O_2, begin decreasing at the edge of preheat zone ($y/L \simeq 0.3$), and react in the reaction zone to form the products, CO_2 and H_2O. The fine structure of counter-flow flame is observed.

To validate the LB simulation, we compare these results with those by conventional method. The distributions of temperature and mass rate of production for propane are shown in Fig. 7. From this figure, wee see that two profiles are perfectly matched and we confirm that LBM is capable of simulating the combustion field.

4.3. Flame Temperature

Next, we examine the flame temperature, which is an important feature of the flame. As seen in the flame structure in Figs. 5 and 6, the maximum temperature is located at the centerline ($y=0$) and is almost constant. Then, we define this maximum temperature as flame temperature, T_f. We compare the flame temperatures obtained by two different schemes, LBM and the conventional method. To examine the compressible effect,

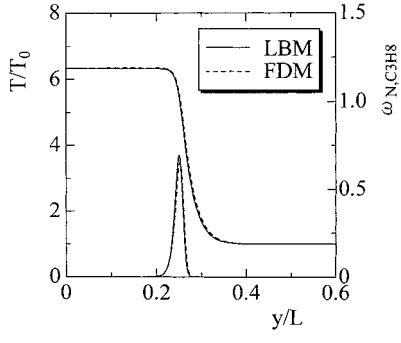

Fig. 7. Distributions of temperature and mass rate of production for propane; $\phi = 0.6$, $\mathrm{Re} = 124$.

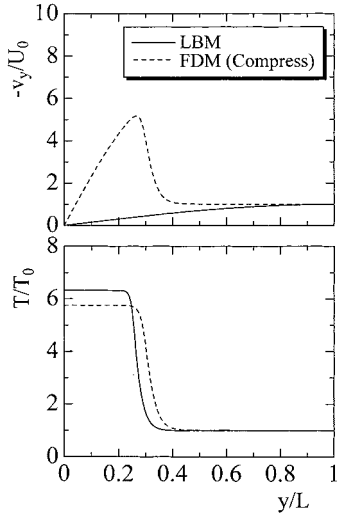

Fig. 8. Distributions of velocity of v_y and temperature; $\phi = 0.6$, Re = 124.

the flow fields by LB method and conventional scheme of the compressible model are compared. Figure 8 shows the distributions of y-direction velocity and temperature. The equivalence ratio is 0.6. It is found that, when the density is changed, the velocity is accelerated due to the flow expansion caused by the increase of temperature. Also, the high temperature region is wider, with lower maximum temperature. Then, we change the fuel concentration of the mixture to increase the equivalence ratio.

Figure 9 shows the variations of the flame temperature, T_f, with equivalence ratio. From this figure, it is seen that the flame temperature

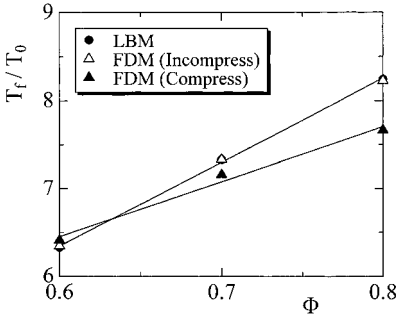

Fig. 9. Variations of flame temperature with equivalence ratio.

monotonically increases with increasing equivalence ratio. This is because the deficient reactant is fuel in the lean mixture and an increase of the fuel concentration results in larger heat release rate. When we compare the temperatures obtained by LBM and incompressible FDM, both results are almost the same. If we take the variable density into account, the calculated flame temperature is slightly decreased. Based on the fact that the temperature difference is larger with an increase of equivalence ratio, the compressible effect is more important as the temperature is larger.

In addition to the compressibility, there is enough room for improvement for better simulation. For example, it is appropriate to use detailed chemistry for predicting the real flame behavior. We may not neglect the variable transport coefficients including heat conduction and diffusion coefficient. Here, we conclude that, by our proposed approach, combustion field can be simulated by Lattice Boltzmann method.

5. CONCLUSIONS

In this present paper, we have proposed the numerical procedure to describe chemical reaction and heat release using an incompressible Lattice Boltzmann model (LBM). We have focused on laminar flame formed in counter flow as a benchmark study. We have assumed that chemical reaction does not affect the flow field for simplicity. To verify our LB model, we solve the governing equations for conservation of mass, momentum, energy, and species by finite difference method. The results of both simulations are in good agreement. If we take the variable density into account, the calculated flame temperature is slightly decreased. Although some improvement may be needed, it is concluded that, the LBM can be used to simulate combustion field.

REFERENCES

1. F. A. Williams, *Combustion Theory* (Benjamin Cummings, Redwood City, 1985).
2. N. Peters, *Proceeding of the Combustion Institute* **21**:1231–1250 (1986).
3. S. Chen and G. D. Doolen, *Annual Reviews of Fluid Mech.* 329–364 (1998).
4. X. He and G. D. Doolen, *Phys. Rev. E* **56-1**:434–440 (1997).
5. D. O. Martinez, W. H. Matthaeus, S. Chen, and D. C. Montgomery, *Phys. Fluids* **6**:1285–1298 (1994).
6. S. Chen, D. O. Martinez, and R. Mei, *Phys. Fluids* **8**:2527–2536 (1996).
7. S. Succi, G. Bella, and F. Papetti, *J. Sci. Comput.* **12-4**:395–408 (1997).
8. K. K. Kuo, *Principles of Combustion* (John Wiley and Sons, New York, 1954).
9. O. Filippova and D. Hanel, *J. Comput. Phys.* **158**:139–160 (2000).
10. H. Tsuji and I. Yamaoka, *Proceeding of the Combustion Institute* **19**:1533–1540 (1982).
11. S. Ishizuka and C. K. Law, *Proceeding of the Combustion Institute* **19**:1541–1548 (1982).

12. M. D. Smooke and V. Giovangigli, *Lecture Notes in Physics*, Vol. 241 (Springer-Verlag, 1985), pp. 1–28.
13. P. A. Libby, N. Peters, and F. A. Williams, *Combust. Flame* **75**:265–280 (1989).
14. K. Yamamoto, *Combust. Flame* **118**:431–444 (1999).
15. C. K. Westbrook and F. L. Dryer, *Combust. Sci. Technol.* **27**:31–43 (1981).
16. D. R. Stull and H. Prophet, *JANAF Thermodynamic Tables*, NSRDS-NBS **37** (National Bureau of Standards, Washington, D.C., 1971).
17. J. O. Hirshfelder, C. F. Curtis, and R. B. Bird, *Molecular Theory of Gases and Liquids* (John Wiley and Sons, New York, 1954).
18. X. He and Li-Shi Luo, *J. Statist. Phys.* **88**(3/4):927–944 (1997).
19. R. J. Kee, J. A. Miller, and T. H. Jefferson, *Sandia National Laboratories Report*, SAND83-8209 (1983).
20. X. He, S. Chen, and G. Doolen, *J. Comput. Phys.* **146**:282–300 (1998).
21. I. Yamaoka and H. Tsuji, *Proceeding of the Combustion Institute* **20**:1883–1892 (1984).